

Geophysical Research Letters
Supplementary Information for

La Niña's Diminishing Fingerprint on the Central Indian Summer Monsoon

**Dhrubajyoti Samanta^{1,*}, Balaji Rajagopalan^{2,3}, Kristopher B. Karnauskas^{3,4},
Lei Zhang⁴, and Nathalie F. Goodkin^{1,5,6}**

¹Asian School of the Environment, Nanyang Technological University, Singapore

²Department of Civil Environmental and Architectural Engineering, University of Colorado Boulder,
USA

³Cooperative Institute for Research in Environmental Science, University of Colorado Boulder,
USA

⁴Department of Atmospheric and Oceanic Sciences, University of Colorado Boulder, USA

⁵Earth Observatory of Singapore, Singapore

⁶Department of Earth and Planetary Sciences, American Museum of Natural History, USA

*Corresponding author: dhruba@ntu.edu.sg or dhruba.samanta@hotmail.com

Contents of this file

Table S1
Figures S1 to S11

Set No.	Experiment name	Tropical Pacific Ocean (30°S-30°N, 120°E-65°W)	Tropical Indian Ocean (IO) (30°S-30°N, 30°E-120°E)
1	Control	Climatology across all oceans	
2	Pre_Pac	pre-1980 La Niña	climatology
2	Post_Pac	post-1980 La Niña	climatology
3	Postpac_IO0.5	post-1980 La Niña	0.5 °C
3	Postpac_IO1.0	post-1980 La Niña	1.0 °C
3	Postpac_IO1.5	post-1980 La Niña	1.5 °C
3	Postpac_IO2.0	post-1980 La Niña	2.0 °C
3	Postpac_IO2.5	post-1980 La Niña	2.5 °C
3	Postpac_IO3.0	post-1980 La Niña	3.0 °C
3	Postpac_IO4.0	post-1980 La Niña	4.0 °C

Table S1. AGCM experiments details with the set number (1st column), experiment name (2nd column), La Niña anomalies applied over the tropical Pacific Ocean (3rd column) and tropical Indian Ocean condition in the simulation (4th column). The digits in the 4th column indicate the magnitude of uniform SST warming (in °C) added over the tropical Indian Ocean in set-3. Monthly SST anomalies and warming applied on top of monthly climatologies based on the 1950-2016 period.

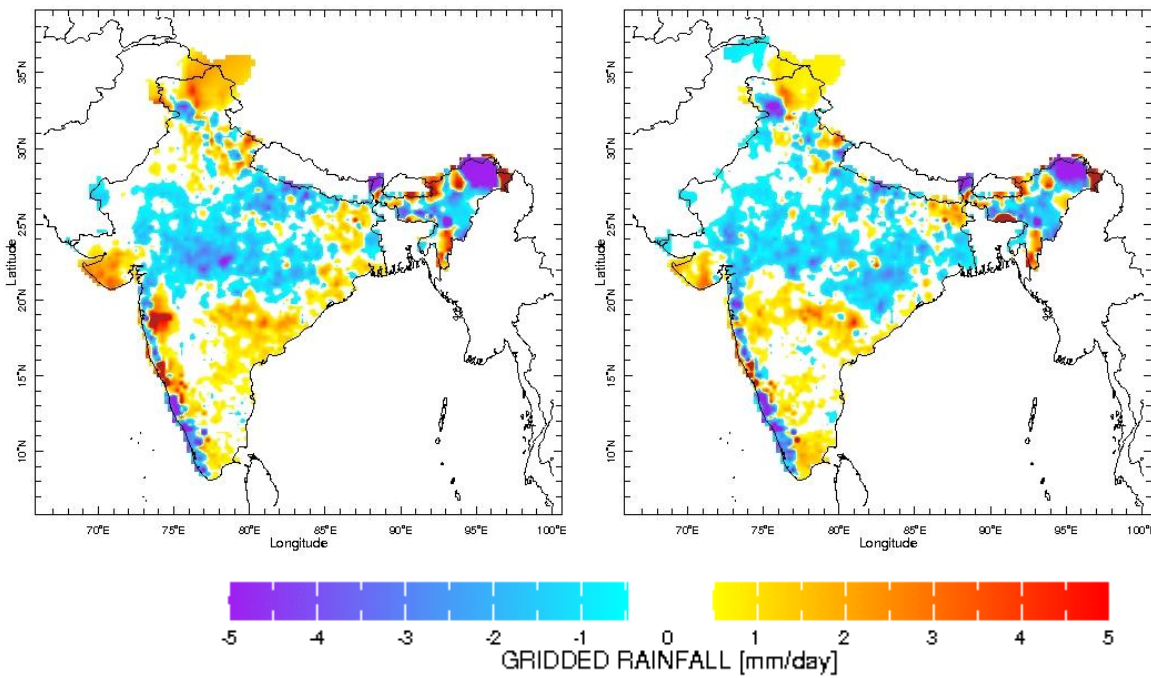


Figure S1: ISM (JJAS) rainfall changes (in $\text{mm} \cdot \text{day}^{-1}$) during post-1980 La Niña period relative to pre-1980 La Niña using IMD data. ISM rainfall changes based on (left) La Niña years from the present study, and (right) La Niña years based on sea surface temperature anomalies for each month of the monsoon season (Gill et al., 2015).

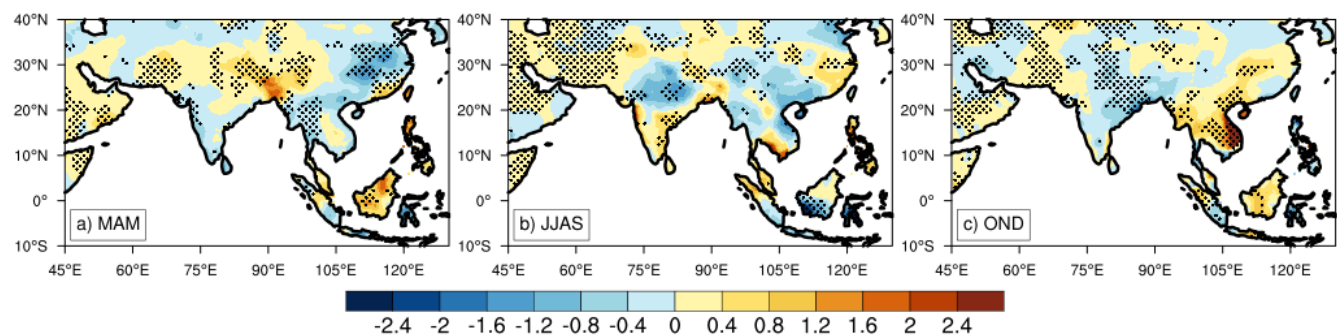


Figure S2: Same as Figure 1a-c, but excluding the cooccurring Indian Ocean Dipole years (1975, 1998, and 2005). Indian Ocean Dipole years were selected based on Hameed (2018).

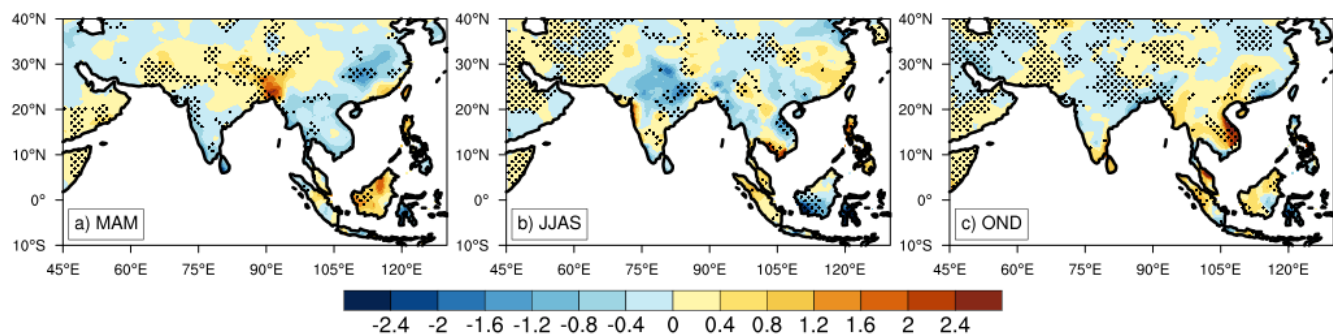


Figure S3: Same as Figure 1a-c, but excluding the stronger La Niña years 1973 and 1998 for the composite analysis. Stronger La Niña years were selected for which 3-month averaged ONI index exceeded -1.75°C .

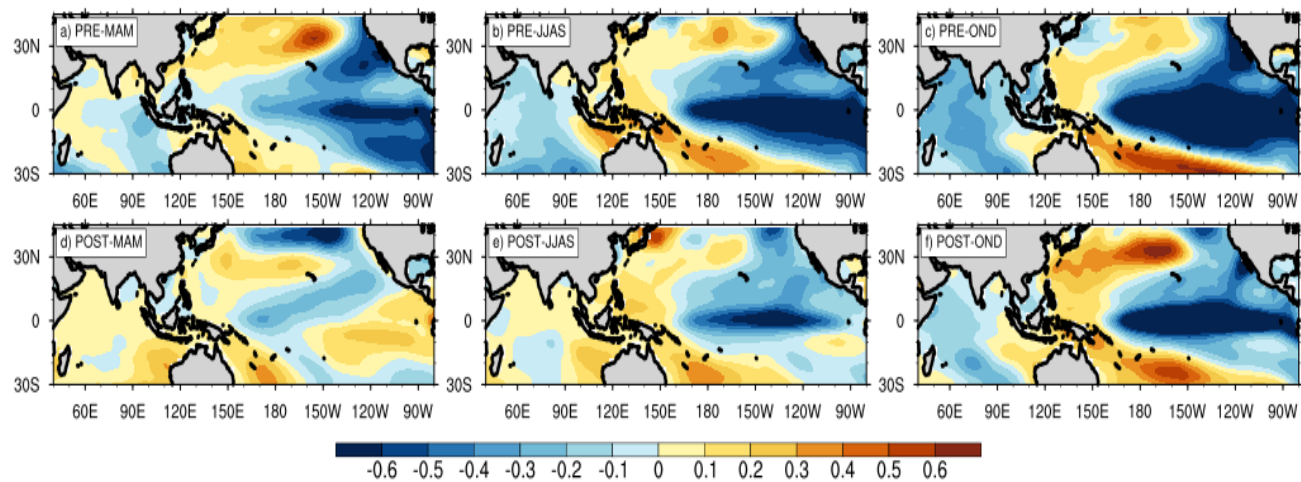


Figure S4: Composite seasonal SST anomaly (in $^{\circ}\text{C}$) during (a-c) pre-1980 La Niñas and (d-f) post-1980 La Niñas. Anomaly is calculated relative to 1950-2016 climatology after detrending the SST time series. Seasons are mentioned in the legend. MAM=March-April-May, JJAS=June-July-August-September, and OND=October-November-December.

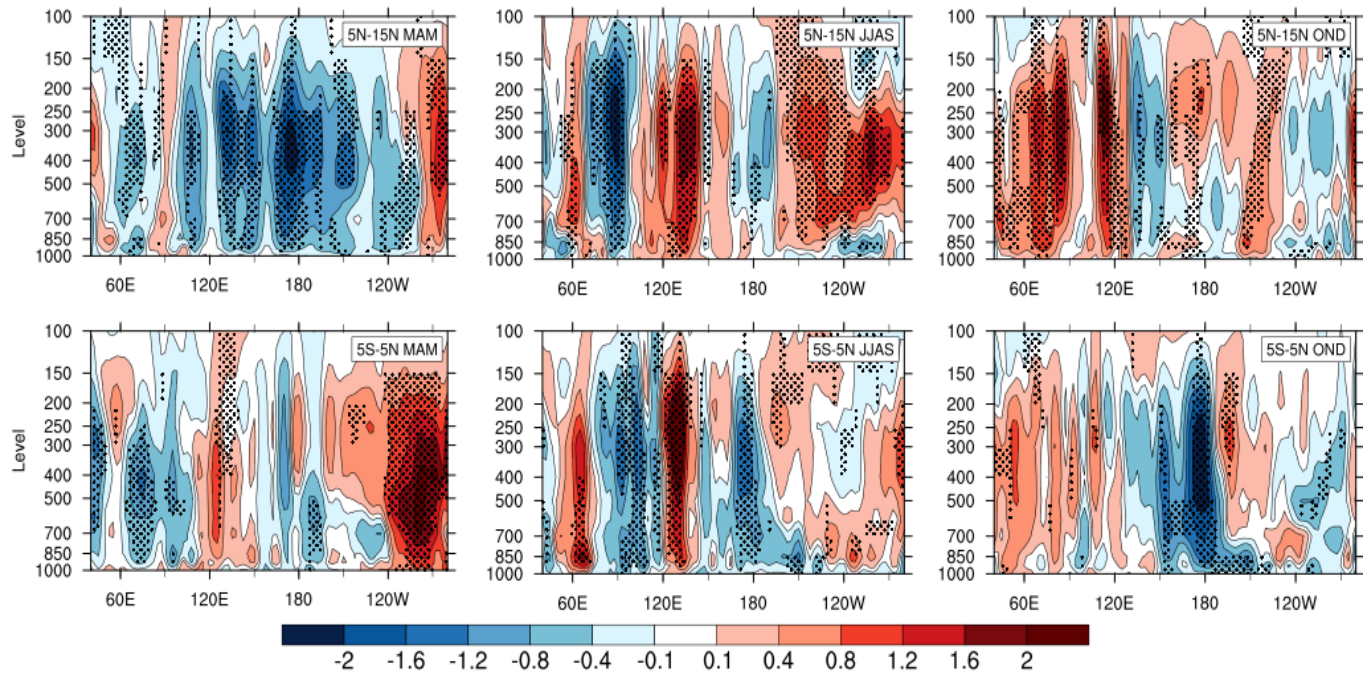


Figure S5: Observed seasonal changes (post-1980 La Niñas minus pre-1980 La Niñas) in east-west circulation patterns. Vertical velocity changes (in 10^{-2} Pa.s $^{-1}$, +ve upwards) averaged over 5°N-15°N (top panel) and 5°S-5°N (bottom panel). Dotted regions indicate 95% confidence level in the changes. Seasons are mentioned in the legend. MAM=March-April-May, JJAS=June-July-August-September, and OND=October-November-December.

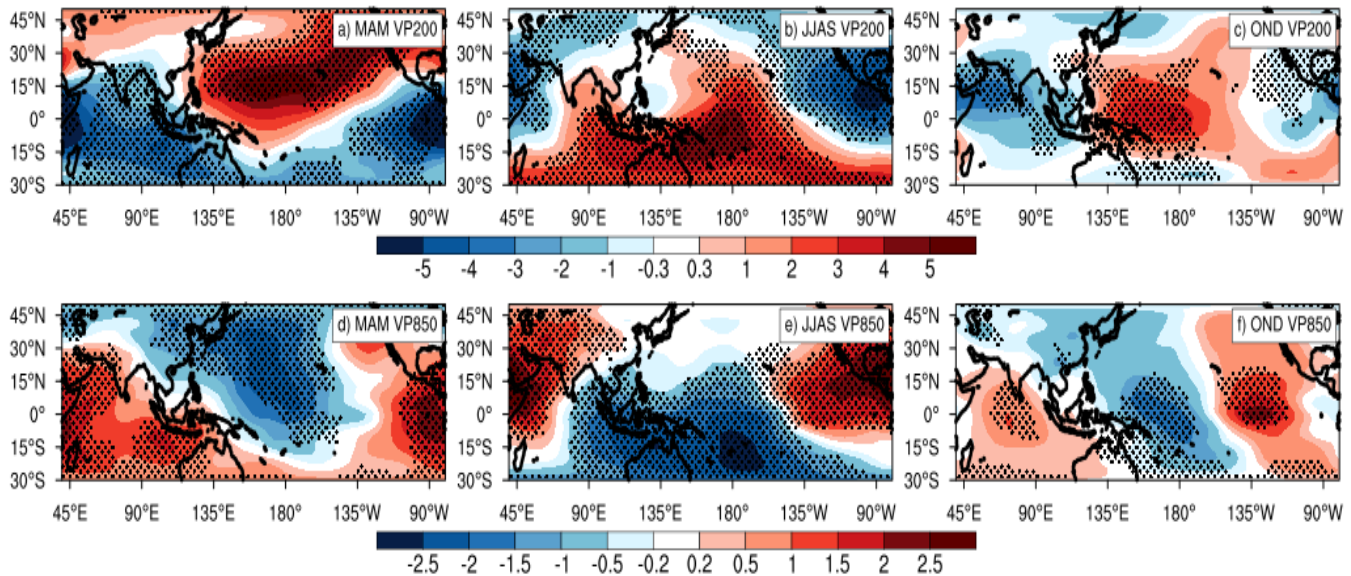


Figure S6: Observed seasonal changes (post-1980 La Niñas minus pre-1980 La Niñas) in velocity potential (VP, in $10^7 \text{ m}^2 \cdot \text{s}^{-1}$). VP for (a-c) 200 hPa, and (d-f) 850 hPa level. Dotted regions indicate 95% confidence level in the changes. Seasons are mentioned in the legend. Seasons are mentioned in the legend. MAM=March-April-May, JJAS=June-July-August-September, and OND=October-November-December.

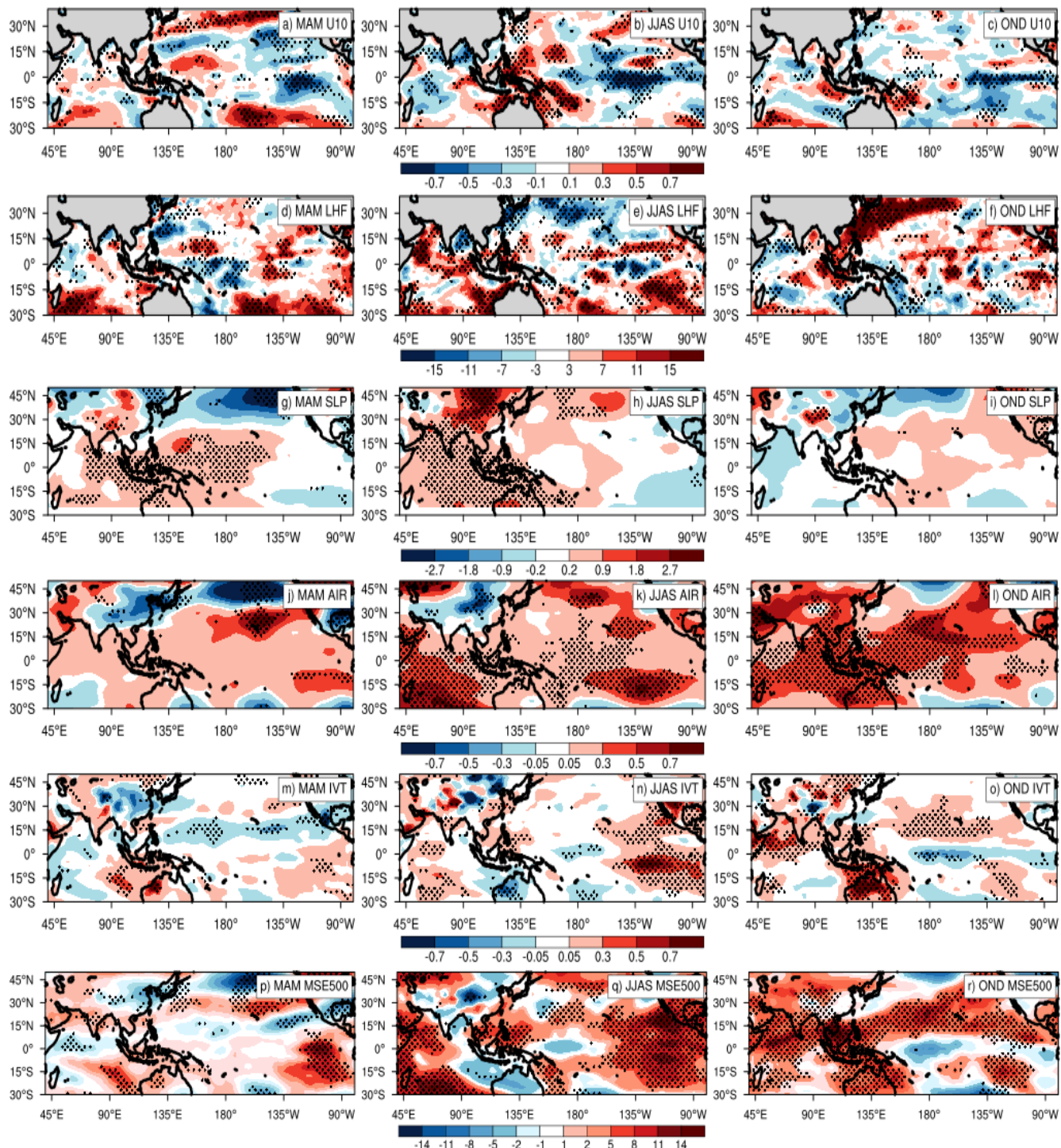


Figure S7: Observed seasonal changes (post-1980 La Niñas minus pre-1980 La Niñas) in air-sea interactions and moisture availability. Seasonal changes in (a-c) 10 m wind speed (u10, in m.s^{-1}), (d-f) latent heat flux (LHF, in W.m^{-2}), (g-i) mean sea level pressure (SLP, in hPa), (j-l) vertical integrated (averaged over 400-700 hPa) air temperature (AIR, in $^{\circ}\text{C}$), (m-o) integrated vapor transport (IVT, in $10^{-1} \text{ kg.m}^{-1}.\text{s}^{-1}$), and (p-r) moist static energy (MSE) at 500 hPa (in $\times 100 \text{ kJ.kg}^{-1}$). Dotted regions indicate 95% confidence level in the changes. Seasons are mentioned in the legend. MAM=March-April-May, JJAS=June-July-August-September, and OND=October-November-December.

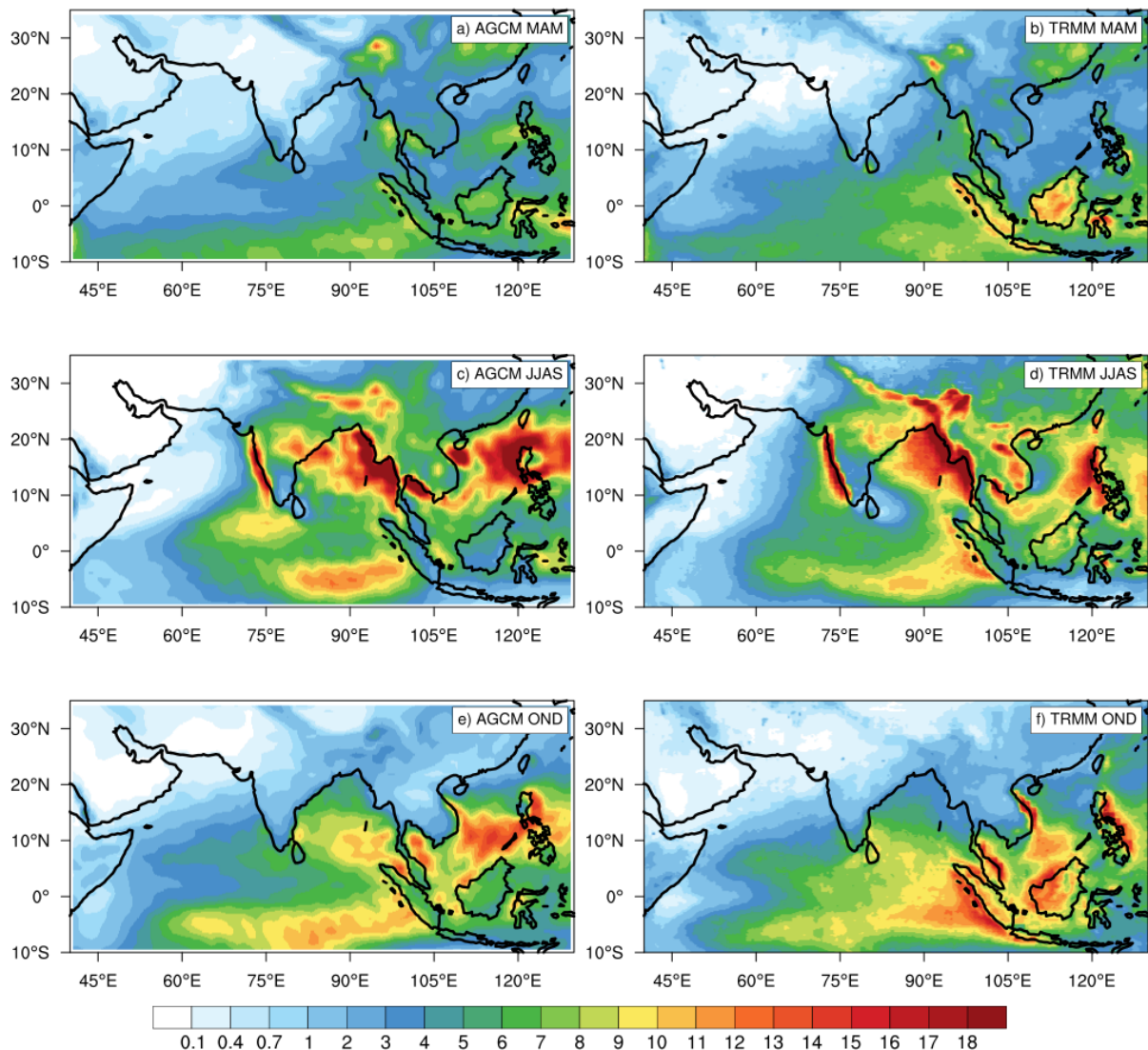


Figure S8: Comparison of seasonal climatological rainfall (in $\text{mm} \cdot \text{day}^{-1}$) between AGCM simulations and observations. Seasonal climatological rainfall for (a,c,e) AGCM control simulations, and (b,d,f) satellite observations (TRMM 3B43). Seasons are mentioned in the legend. MAM=March-April-May, JJAS=June-July-August-September, and OND=October-November-December. Monthly TRMM 3B43 data during 1998-2018 was downloaded from

https://disc2.gesdisc.eosdis.nasa.gov/s4pa/TRMM_L3/TRMM_3B43.7/.

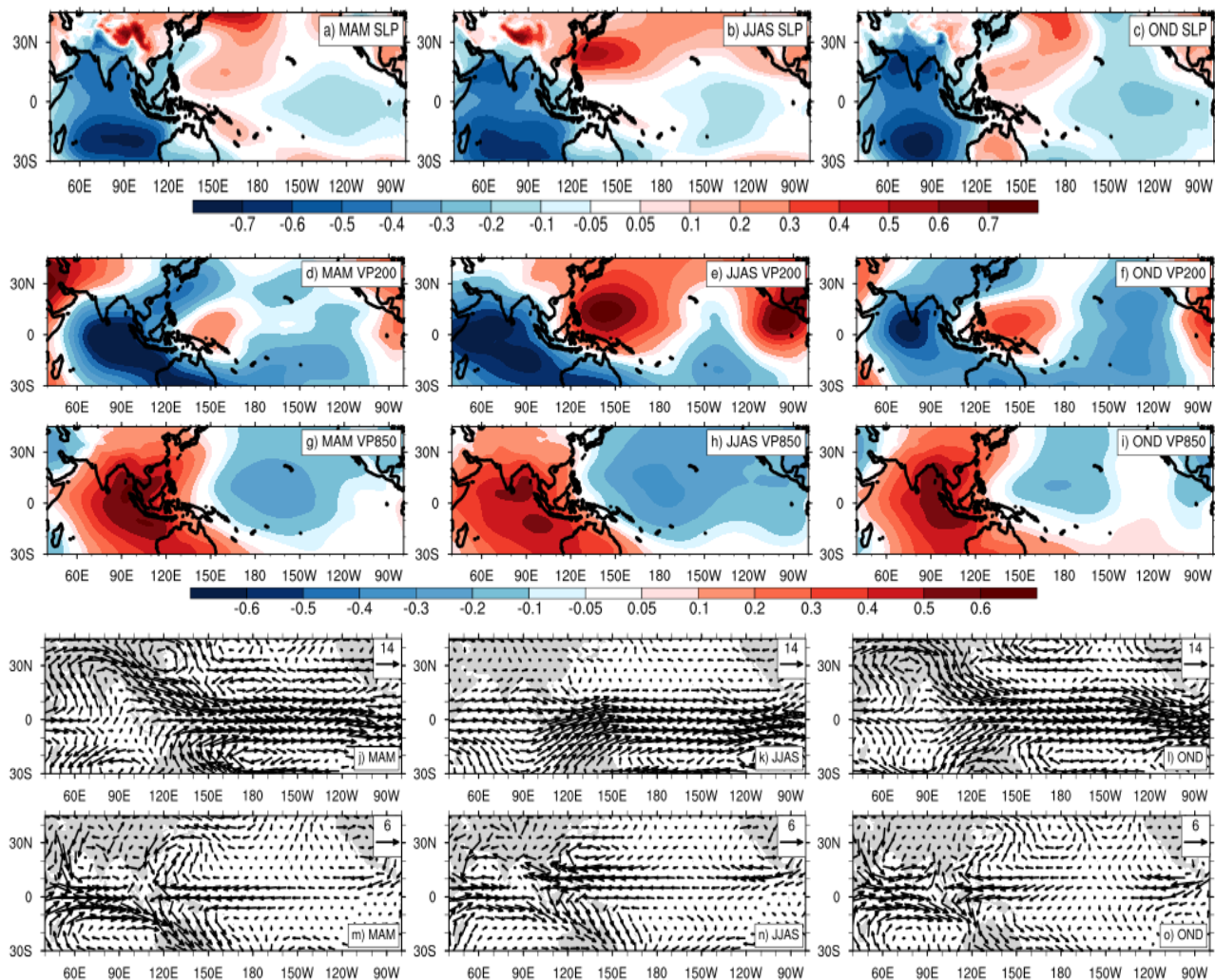


Figure S9: Seasonal changes in large-scale patterns due to 3 °C tropical Indian Ocean warming (i.e., 3 °C set-3 experiment minus control experiment). Seasonal changes in (a-c) sea level pressure (SLP; in hPa), (d-f) 200 hPa velocity potential (VP200, in $10^7 \text{ m}^2 \cdot \text{s}^{-1}$), (g-i) same as d-f, but at 850 hPa, (j-l) 200 hPa wind pattern (in $\text{m} \cdot \text{s}^{-1}$), (m-o) same as (j-l), but at 850 hPa. Seasons are mentioned in the legend. MAM=March-April-May, JJAS=June-July-August-September, and OND=October-November-December.

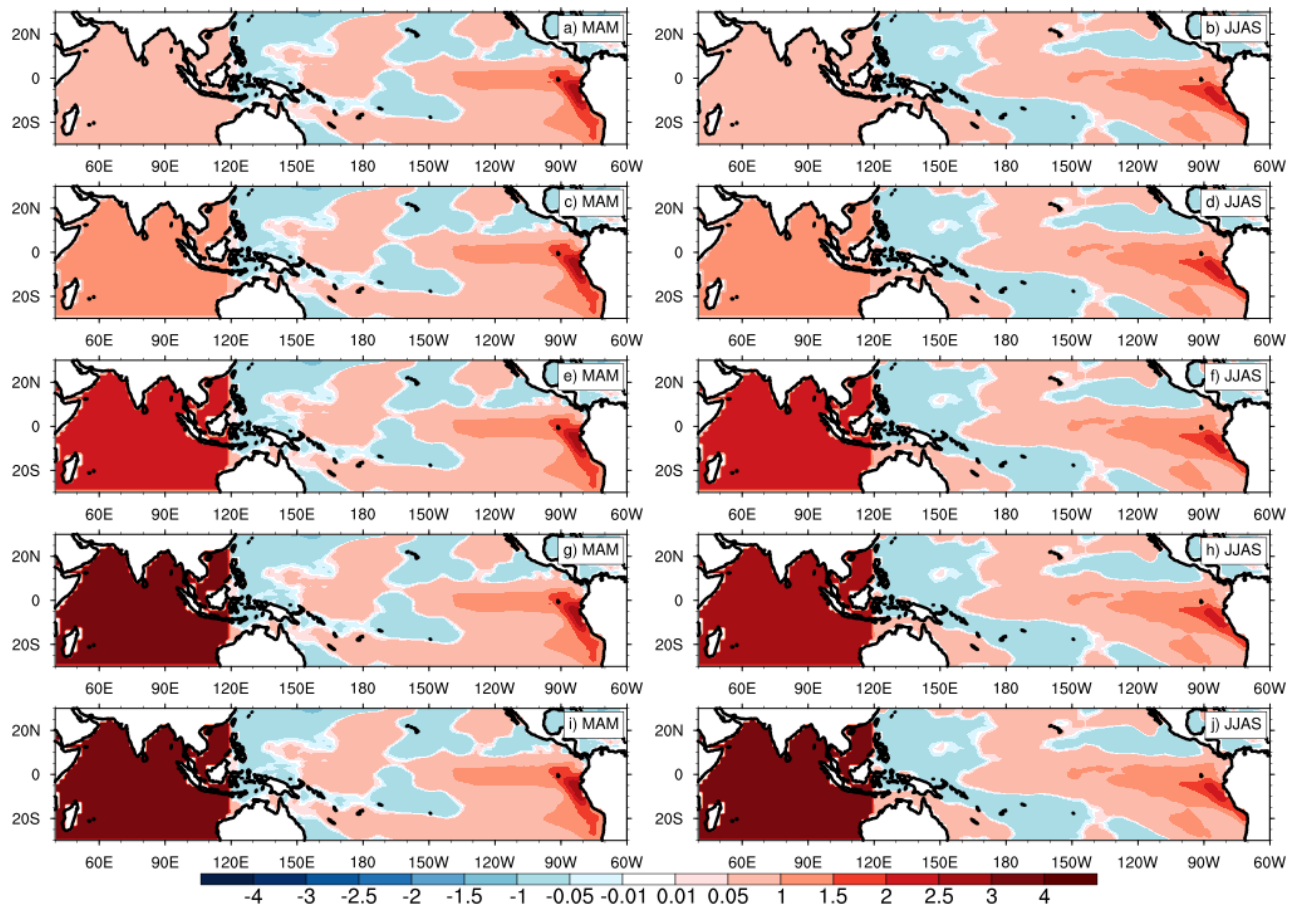


Figure S10: SST forcing for set-3 AGCM experiments. Seasonal SSTs (in °C) relative to Pre-Pacific experiment SST forcing for (a-b) 0.5°C, (c-d) 1.0°C, (e-f) 2.0°C, (g-h) 3.0°C, and (i-j) 4.0°C IO warming experiments in set-3. Seasons are mentioned in the legend. MAM=March-April-May, JJAS=June-July-August-September.

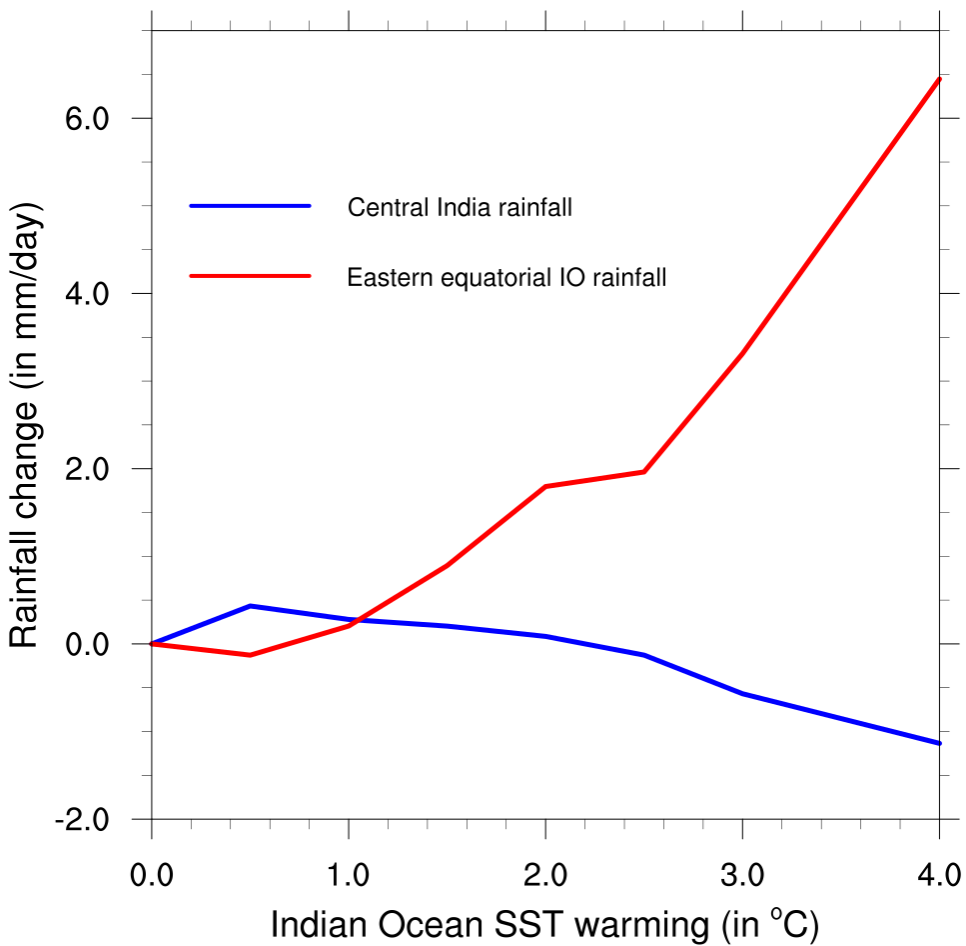


Figure S11: Rainfall changes (in $\text{mm} \cdot \text{day}^{-1}$) with increasing tropical Indian warming from set-3 AGCM simulations. Central India and eastern equatorial Indian Ocean (IO) (5°S - 5°N , 75°E - 95°E) rainfall during monsoon season (JJAS) as a function of an increase in basin-wide tropical Indian Ocean warming up to 4°C from the set-3 AGCM simulations. The rainfall change is relative to Post-Pac experiment (i.e. post-1980 La Niña tropical Pacific SST condition).